Primljen / Received: 3.4.2022.
Ispravljen / Corrected: 5.9.2022.
Prihvaćen / Accepted: 26.12.2022.
Dostupno online / Available online: 10.2.2023.

Performance of reinforced engineered cementitious composite square columns

Authors:

Mohsen Dayyani, PhD candidate
Islamic Azad University, Tehran, Iran
Central Tehran Branch
Department of Civil Engineering
dayyanimohsen@gmail.com

Assoc.Prof. **Alireza Mortezaei**, PhD. CE
Islamic Azad University, Semnan, Iran
Semnan Branch
Department of Civil Engineering
a.mortezaei@semnaniau.ac.ir
Corresponding author

Assist.Prof. **Mohammad Sadegh Rohanimanesh**
Islamic Azad University, Tehran, Iran
Central Tehran Branch
Department of Civil Engineering
m.s.rohanimanesh@iauctb.ac.ir

Assist.Prof. **Jafar Asgari Marnani**, PhD. CE
Islamic Azad University, Tehran, Iran
Central Tehran Branch
Department of Civil Engineering
j_asgari@iauctb.ac.ir

Research Paper

Mohsen Dayyani, Alireza Mortezaei, Mohammad Sadegh Rohanimanesh, Jafar Asgari Marnani

Performance of reinforced engineered cementitious composite square columns

This paper investigates the effects of aspect ratio and fibre fraction on the failure of engineered cementitious composite (ECC) concrete columns. When subjected to cyclic load, these columns may fail due to the strain-hardening of longitudinal bars or the formation of dominant cracks. In this experiment, 11 ECC columns with fibre fractions between 0–1.5 % and aspect ratios from 3–7, as well as a single reinforced concrete column, were tested. The results showed that both aspect ratio and fibre fraction significantly impacted the failure paths observed. Additionally, the ECC columns exhibited a cumulative energy dissipation capacity approximately 100 % higher than that of the conventional concrete column.

Key words:
engineered cementitious composite, square column, fibre fraction, aspect ratio, failure path

Prethodno priopćenje

Mohsen Dayyani, Alireza Mortezaei, Mohammad Sadegh Rohanimanesh, Jafar Asgari Marnani

Ponašanje armiranobetonskih kvadratnih stupova od mikroarmiranih cementnih kompozita

Ovaj rad istražuje učinke geometrijskih omjera i udjela vlakana na slom betonskih stupova od mikroarmiranih cementnih kompozita visokih performansi (eng. *engineered cementitious composite* - ECC). Kada su podvrgnuti cikličnom opterećenju, ti stupovi mogu otkazati zbog očvršćivanja uzdužne armature ili stvaranja dominantnih pukotina. U ovom je istraživanju ispitano 11 ECC stupova, s udjelom vlakana između 0-1,5 % i omjerom duljine stupa i visine presjeka (geometrijski omjer) od 3 do 7, te jedan standardni armiranobetonski stup. Rezultati su pokazali da su i geometrijski omjer i udio vlakana značajno utjecali na uočene mehanizme sloma. Nadalje, ECC stup je demonstrirao kapacitet kumulativne disipacije energije koji je bio približno 100 % veći nego kod konvencionalnog betonskog stupa.

Ključne riječi:
projektirani cementni kompozit, kvadratni stup, udio vlakana, geometrijski omjer, mehanizam sloma

1. Introduction

An ECC (engineered cementitious composite) is a type of fibre-reinforced concrete (FRC) that contains dispersion fibres in a cementitious matrix and exhibits strain-hardening behaviour. FRCs also exhibit a tension-softening behaviour when carrying a load [1, 2]. ECCs are ductile, and their tensile strain capacity typically exceeds 2 % [3, 4]. Some prominent characteristics of reinforced ECCs make them more suitable for use in structural members than conventional concrete [5]. Two failure paths have been recognized by researchers: one involves the localization of cracks and the other occurs by strain-hardening in longitudinal bars [6]. This study illustrated the effect of fibre fraction (0–1.5 %) and aspect ratio (3–7) on the failure path. The advantages of ECCs in terms of safety, sustainability, stability, and economy have promoted their use in the infrastructure and building industry while encouraging engineers to investigate the most prominent characteristic of resilient members, i.e., their delay in failure, exhibited by ECC elements when severe loads are applied. Thus, ECC elements enhance structural functionality [7]. Parra-Montesinos et al. studied hybrid beam-column connections that exhibited inelastic behaviour. These connections comprised a steel beam and reinforced concrete (RC) column, with seismic loading applied. Further, they noted that substituting ECC for conventional concrete without transverse bars generated the highest bond efficiency [8]. Fischer and Li examined steel/ECC and FRP/ECC beams and columns in a self-centring and moment-resisting frame [9].

A literature review of previous studies suggests that only a few studies have focused on structural ECC members and the seismic behaviour and failure paths of ECC square columns. Most studies on this topic have focused on using ECCs as auxiliary material for strengthening or rehabilitating all or part of concrete or masonry structural components. The load-carrying capacity of an ECC specimen depends on fibre bridging. If the fibre bridging completely pulls out or ruptures (or a combination of both), then the specimen's load-carrying capacity is lost. If the bridging capacity is larger than the remaining steel, the cracks will be localized [10–12]. ECC flexural members can fail in two different manners under load [13]: the first occurs when one or more dominant cracks form, while the second occurs when the longitudinal reinforcing steel undergoes strain-hardening. The first path cannot compensate for the load capacity by hardening the longitudinal reinforcing steel, while the second path increases the load capacity as the steel undergoes strain-hardening [14–16]. These two failure paths are investigated based on different fibre fractions (0–1.5 %) and aspect ratios (3–7). Previous studies have limited the fibre fraction to 2 %; however, this study examines the effect of a wider range of fibre fractions and aspect ratios on the failure paths.

2. Experimental methods

2.1. Materials

Researchers have utilized ECCs in various structures, such as buildings and bridges [14]. In the laboratory, mixture design and sample tests were conducted, as presented in Table 1 and Figure 1. The ECC concrete matrix contained polyvinyl alcohol (PVA) fibres, shown in Table 2 (length = 8 mm, volume fraction = 0-1.5 %) and made of Type II cement and class F fly ash in accordance with EN450 and BS3892, as well as #50 silica sand.

Table 2. Specifications of the polyvinyl alcohol

Fibre name	RCS15
Manufacturer	Nycon
Material	PVA
Configuration	Resin-bundled chopped fibre
Colour	White or yellowish-white
Specific gravity	1.3
Length	1/3" (8 mm)
Tensile strength	210 ksi (1400 MPa)
Flexural strength	4200 ksi (30 GPa)
Water absorption	<1 % by weight
Alkali resistance	Excellent
Concrete surface	Non-fuzzy
Corrosion resistance	Excellent

This matrix also included a viscosity-modifying admixture (VMA) and a high-range water-reducing (HRWR) admixture. According to ASTM C494, the compressive strength of conventional concrete was similar to that of the ECC mixture. The size of coarse aggregates in conventional concrete was limited to 9.5 mm. The properties of the reinforcing steel are depicted in Table 3. In this study, six samples were initially designed to verify the compression strength and other parameters related to the ECC admixture, including using five different fibre fractions (0 to 1.5 %) and a single conventional concrete specimen. Ultimately, 12 cubic compression specimens (six bending specimens and six Brazilian splitting tensile specimens) were tested according to ASTM standards. Several cubic concrete and ECC specimens (100 x 100

Table 1. Mixture compositions of the test specimens by cement weight ratio [17]

Matrix	Cement	Fly ash	Coarse aggregate	Fine aggregate	Water	VMA (% wt. cement)	HRWR (% wt. cement)	PVA (% volume)
ECC	1.0	1.2	0	0.8	0.63	0.12	0.5	0-1.5
Beton	1.0	0	1.14	1.05	0.40	0	0	0

Table 3. Properties of the reinforcement steel

Diameter [mm]	Area [mm^2]	Yield strength [MPa]	Ultimate strength [MPa]
10	78.5	475	510
12	113.04	463	542
16	200.96	419	495
18	254.34	465	541
20	314	406	471

Table 4. Specifications of the stress–strain sample

Conducted tests	Foce [N]	Extension [mm]	Stress [MPa]	Elongation [%]	
Bending	Peak	18148.5	4.4682	0.51	4.4682
	Break	2550.6	9.0255	0.0729	9.0255
Brazilian	Peak	438825.9	9.187	9.6234	5.9212
	Break	410327.8	9.2939	8.9984	6.035
Compressive	Peak	333834.3	2.5774	33.3834	2.5774
	Break	226341.2	3.0565	22.6341	3.0565

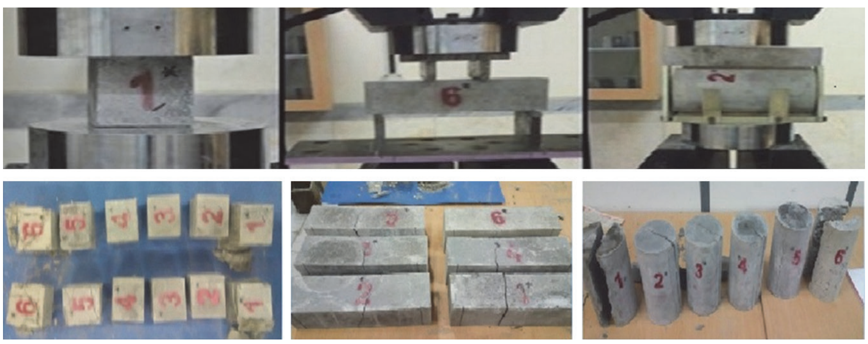

Figure 1. Laboratory samples

x 100 mm) were prepared for compression tests. The estimated compressive strengths of the concrete and ECC were compared by testing the ECC and concrete on different days (28 ±2 days and 56 ±2 days, respectively), allowing the reinforced concrete specimens to cure for longer than the ECC specimens. Their compressive strengths were 34.50 MPa. Figure 2 and Table 4 represent the strain curve of bending, Brazilian, and compressive strength for the 1.5 % fraction of the fibre, respectively.

ECCs typically show uniaxial tensile strain-hardening behaviour, making them suitable for structural-level analysis based on various articles and standards [18]. The properties of the reinforcing steel used in this study are presented in Table 4.

2.2. Specimen design and test setup

Several column specimens were tested to examine the impact of fibre fraction on the failure path of RC and ECC square columns.

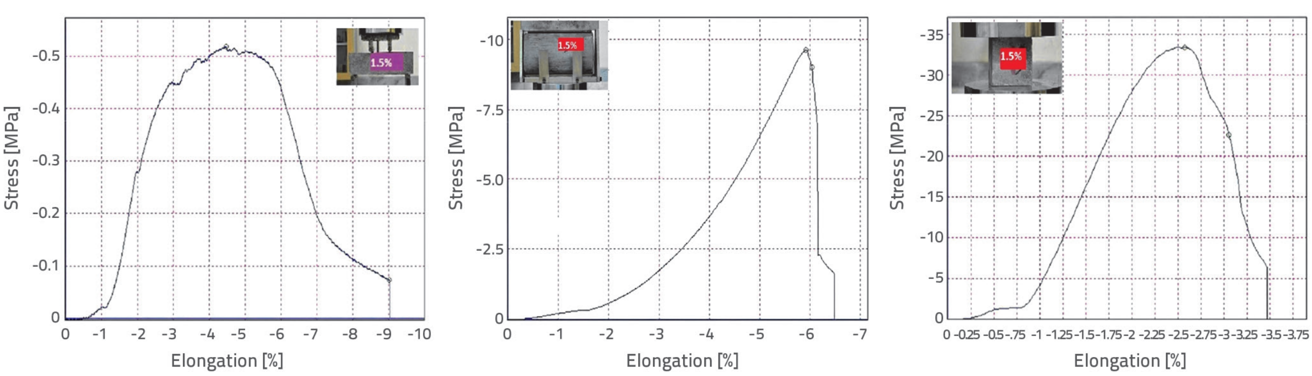

Figure 2. Stress–strain sample

Table 5. Geometry and reinforcement of the column specimens

Specimen	Material	Cross section [mm x mm]	Height [mm]	Aspect ratio	Longitudinal reinforced ratio [%]	Fibre [%]	Longitudinal bars	Transverse bars
SP1	ECC	250 x 250	750	3	1	0	8Φ10	5Φ10
SP2	ECC	300 x 300	900	3	1	0	8Φ12	5Φ10
SP3	ECC	350 x 350	1050	3	1.3	0.3	14Φ12	6Φ10
SP4	ECC	400 x 400	1200	3	1.15	0.3	16Φ12	6Φ10
SP5	RC	400 x 400	1200	3	1.15	0.0	16Φ12	6Φ10
SP6	ECC	200 x 200	1000	5	1.57	0.6	8Φ10	7Φ10
SP7	ECC	250 x 250	1250	5	1.96	0.6	8Φ12	8Φ10
SP8	ECC	350 x 350	1750	5	1.65	0.6	8Φ18	10Φ10
SP9	ECC	300 x 300	1800	6	1.77	1.0	8Φ16	10Φ10
SP10	ECC	350 x 350	2100	6	2.3	1.5	8Φ20	10Φ10
SP11	ECC	200 x 200	1400	7	1.57	1.0	8Φ10	10Φ10
SP12	ECC	250 x 250	1750	7	2.56	1.5	8Φ16	10Φ10

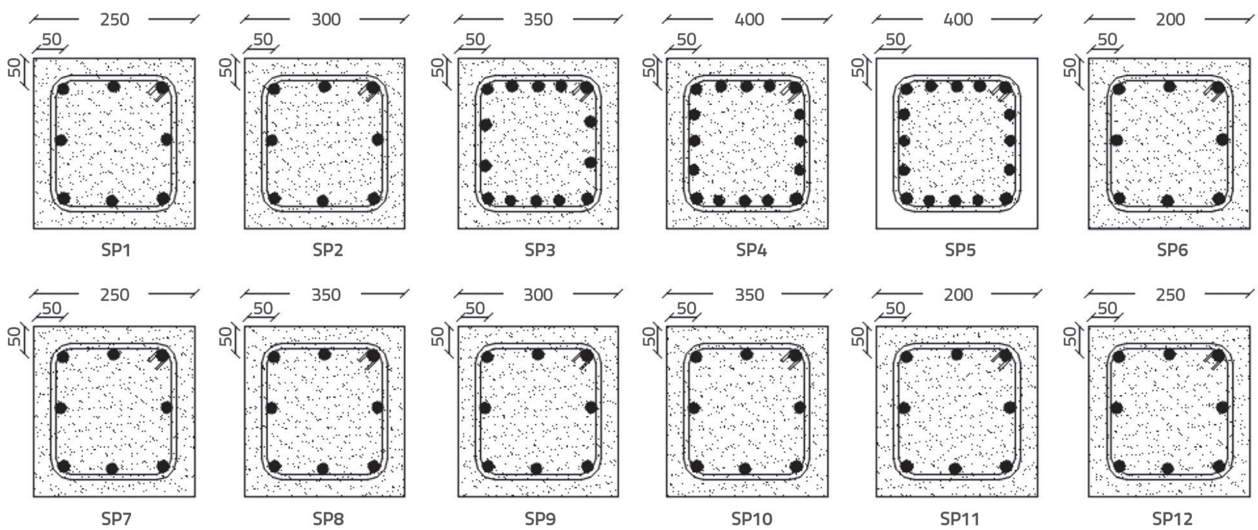

Figure 3. Column reinforcement layouts

As shown in Figure 4, the ECC material was used to cast the connection part of the foundation beam to prevent the weakening of the column-foundation beam interface. The specimen details and layout are presented in Table 5 and Figure 3, respectively. The 12 reinforced concrete specimens were moist-cured for seven days and then left at room temperature to continue curing until the tests were conducted. Longitudinal and transverse bars with six and three strain gauges, respectively, were installed on the concrete at 0.15 H, 0.20 H, and 0.45 H above the joint faces, as shown in Figure 4. In addition, seven concrete strain gauges were also installed.

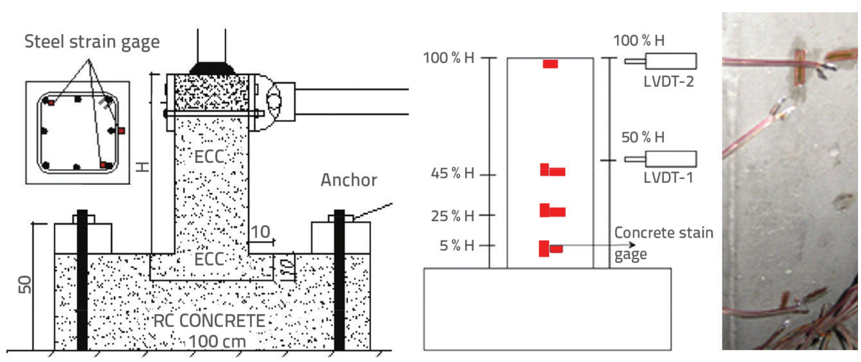

Figure 4. Column specimen manufacturing process

2.3. Test equipment and loading procedure

As shown in Figure 5, the bottom stub of each specimen was fixed to the base to create loading conditions that would result in flexural deformation in all specimens, which helped investigate the impact of the ECC material on the expected plastic hinge region.

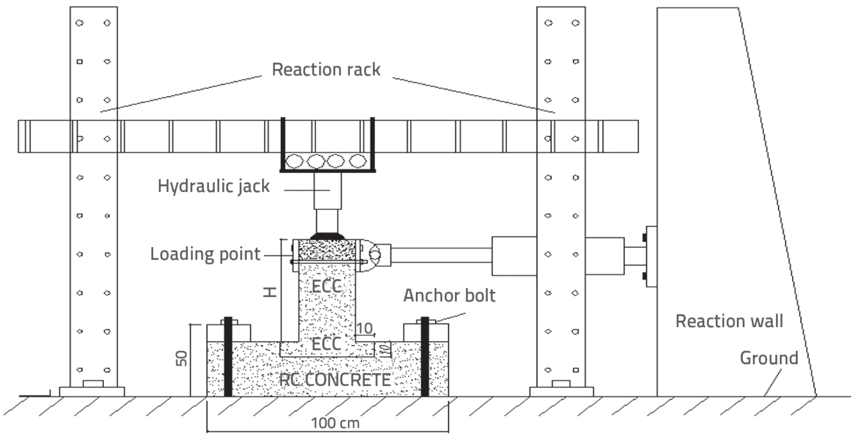

Figure 5. Test setup of the specimens

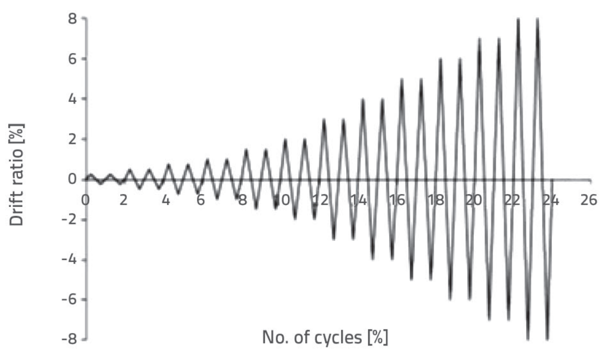

Figure 6. Displacement-controlled protocol [19]

Before horizontal loading was applied, a constant axial load of 20 % of the nominal compressive capacity of the column was applied to the top of the column specimen using a hydraulic jack. A pulley with rollers was installed between the hydraulic jack and the reaction steel beam to reduce friction between the hydraulic jack and the reaction steel frame. In addition, a reaction wall equipped with a 250-kN actuator was used to apply lateral loads. This process was conducted following a predefined displacement controlled loading sequence, with the load manually applied at the peak of each cycle according to the loading protocol shown in Figure 6 [19].

3. Experimental results

3.1. Hysteresis loop

The crack patterns of the 12 columns are depicted in Figure 7. The failure paths (strain-hardening and crack localization) are marked with "X" and "O," respectively, as shown in Figure 8. Specimens SP1, SP2, SP3, and SP5 failed by forming crack localization and dominant cracks. Additionally, SP1 split, spalled, and failed abruptly due to a lack of fibre. The hysteretic response of SP5 exhibits pinching and lower reloading stiffness compared to SP4 and the other ECC specimens. Furthermore, most cracks in SP4 formed after the longitudinal bars experienced strain-hardening and yielding. The dispersed fibres in SP4 eliminated pinching, thereby significantly improving the load capacity and section stiffness more than in SP5. The following two failure paths were observed in this study. The results indicate that SP1, SP2, SP3, and SP5 failed due to cracking localization (splitting and spalling were also observed); the remaining specimens failed after gradual strain-hardening, commonly observed in fibre–concrete samples [20–22]. As they lacked fibre bridging and experienced spalling in the concrete covering the longitudinal bars, specimens SP1, SP2, SP3, and SP5 experienced buckling alongside large longitudinal and severe bond splitting. As shown in Figure 9, a comparison between the hysteresis loop and strain-hardening of the longitudinal bars in SP4 and SP5 reveals that SP4 has a greater stable load envelope compared to SP5. The figure also demonstrates that SP4 absorbs more energy than SP5 due to

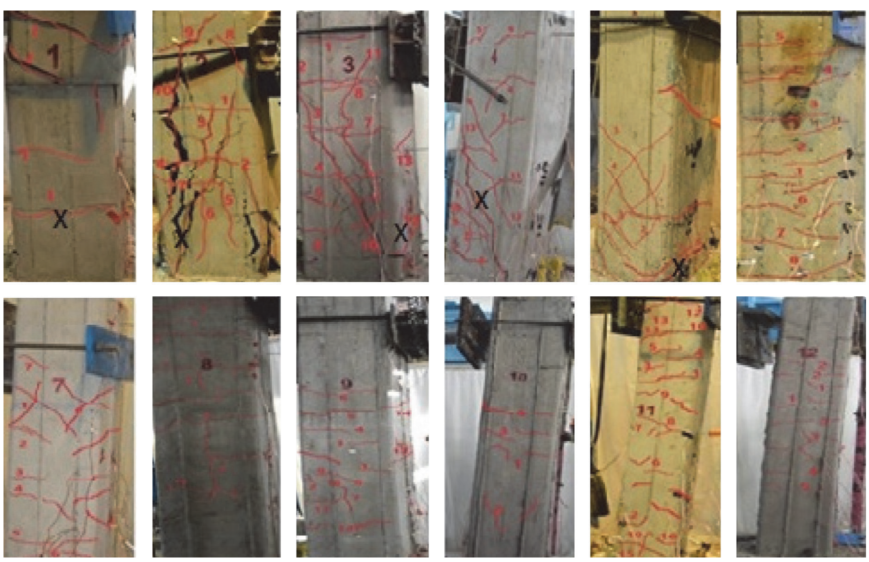

Figure 7. Specimen cracking patterns following failure

its ability to eliminate pinching. The two different failure paths are clearly observed in SP4 (strain-hardening) and SP5 (crack localization).

The load capacities of SP4, SP6, and SP7 slightly increased after the localization of micro-cracks, but they quickly experienced steel strain-hardening before losing their fibre-bridging capacity and, therefore, their load-carrying capacity. These conditions ultimately led to the fracture of the reinforcing steel. The ECC was crushed, causing the longitudinal steel to crack and initiating the failure of SP8, SP9, SP10, SP11, and SP12. Failure drifts of 4.8 % were observed for the conventional columns. With a lower fibre fraction and aspect ratio, the ECC columns demonstrated a smaller drift capacity compared to conventional columns.

When SP5 reached its maximum load of 150 kN (with a corresponding drift of 4.8 %), the concrete was crushed and lost its load capacity. In contrast, SP4's load capacity increased until the fibres began to pull out or rupture as a dominant crack formed due to fibre bridging. The peak load of SP4 is 30 % higher than that of the conventional specimen. Additionally, strain-hardening occurred in SP4 after crack localization and fibre bridging failure. The advantage of strain-hardening failure over crack localization is that the wide cracks indicate impending abrupt failure. The cracking pattern in SP4 is denser and covers more than 80 % of the specimen's height, while the ultimate load integrity of the member was maintained. In contrast, the localized crack in SP5 extended from the base of the column to 35 % of its section height. Increasing the aspect ratio and fibre fraction in ECC columns increases the drift capacity, as confirmed by previous research on reinforced ECCs [23].

The results show that when the fibre fraction of reinforced specimens was increased from 0.3 % to 1.5 %, the failure path changed from crack localization to gradual strain-hardening, resulting in an increase in drift capacity by 79.2 % because the decrease in load capacity caused by the loss of fibre-bridging capacity after crack localization was compensated for by the reinforcing steel's hardening capacity. The increases in peak specimen strength (13 to 15 for SP5 and 18 to 20 for SP4 reinforced ECC) were due to differences in the tension and compression of the ECC and conventional columns (Figure 9). The hysteretic response of the reinforced concrete (SP5) exhibits pinching and lower reloading stiffness, ultimately failing by crushing and spalling (Figure 10), consistent with previous research indicating the high damage tolerance of ECCs [24]. In comparison to SP5, SP4 maintains more residual stiffness, has a higher ultimate drift, and exhibits better resistance to splitting and spalling. Additionally, the failure mode changes from crack localization to strain-hardening when the aspect ratio and fibre fraction are increased. In specimens SP1, SP2, SP3, and SP5, a shear failure is observed due to crack localization and longitudinal bars remaining in the elastic stage. In SP4, SP6, SP7, SP8, SP9, and SP11, the strain-hardening of longitudinal bars increases significantly, and the failure path changes from shear to flexural shear. Finally, by increasing the aspect ratio and fibre fraction in SP10 and SP12, fine cracks spread throughout the samples, and flexural failure is observed. Therefore, when the failure

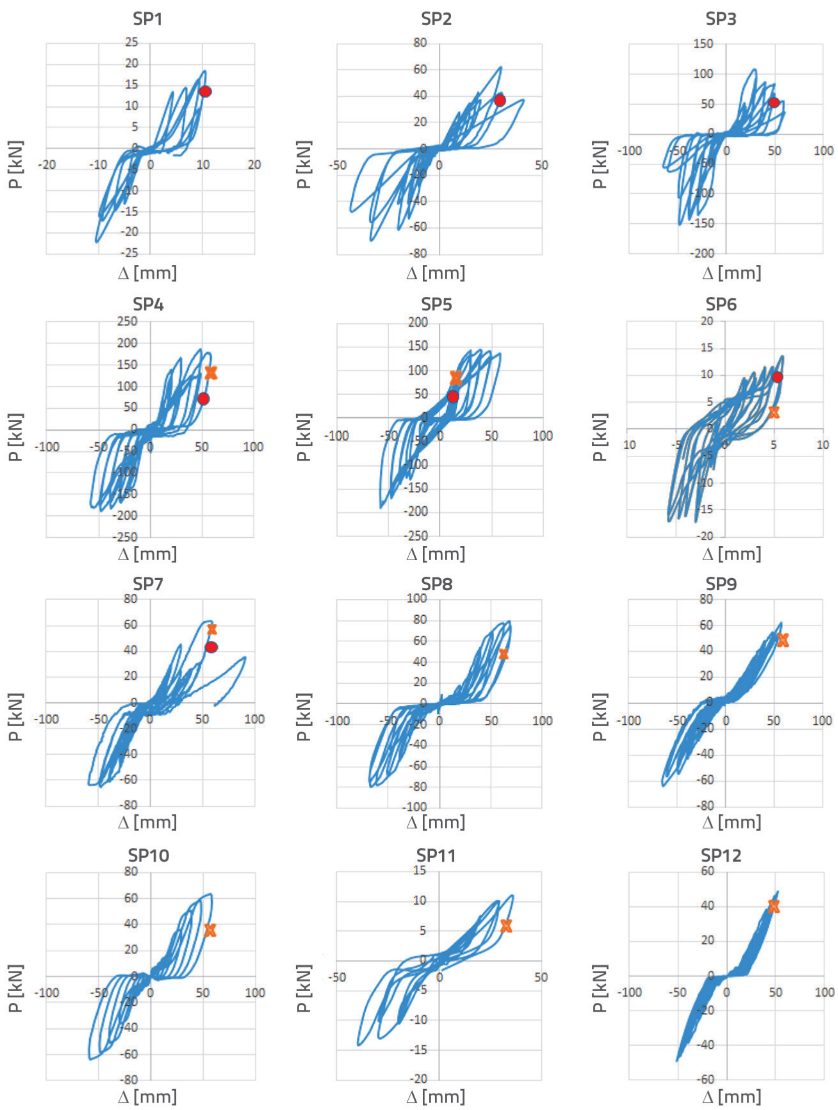

Figure 8. Hysteresis curves of the test specimens

path changes from crack localization to strain-hardening by increasing the fibre fraction and aspect ratio, the failure of the column occurs by shear, shear flexural, and flexural failure, respectively.

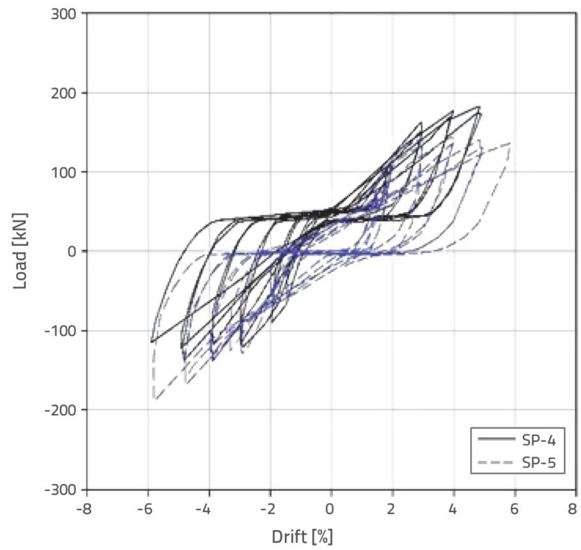

Figure 9. Hysteresis loops of SP4 (ECC) and SP5 (RC)

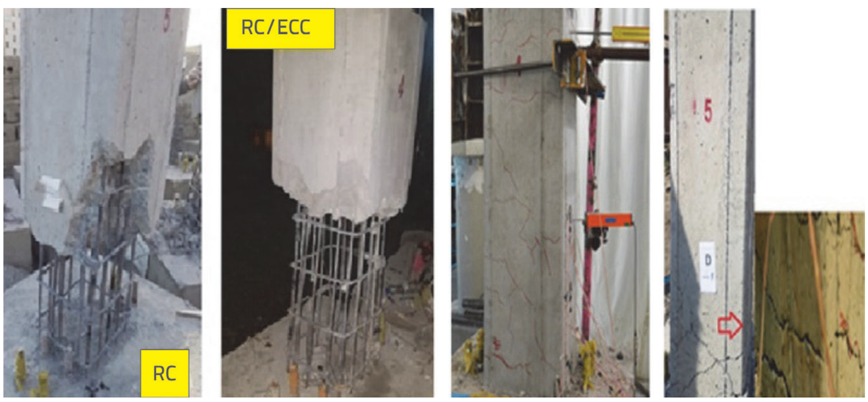

Figure 10. Failure patterns of SP4 (ECC) and SP5 (RC)

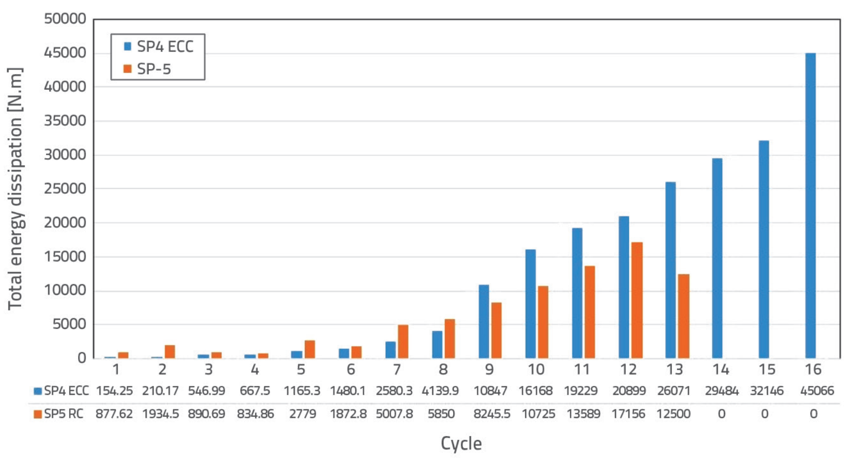

Figure 11. Cumulative energy dissipation capacity of test specimen

3.2. Energy dissipation

Figure 11 displays cumulative energy dissipation capacity in each loading cycle according to ASCE41-13 [25]. This capacity was measured until the end of the test for some specimens. In most ECC specimens, the cumulative energy dissipation capacity significantly increased as the loading cycle was increased once the maximum strength was reached. The cumulative energy dissipation capacity for SP4 was approximately 100 % higher than that of SP5, indicating that using fibres help increase bridging where the cumulative energy is dissipated by repeating the loading cycles. The strain gauge, which monitors the transverse bars, remains in elastic status, indicating the proper performance of the ECC specimens and demonstrating that the transverse reinforcement did not significantly affect the ECC specimen's energy dissipation.

3.3. Plastic hinge

During severe earthquakes, the performance of concrete members is nonlinear, and this nonlinear behaviour, particularly in RC columns, is recognized as the yield region. In the yield region, longitudinal steel yields, concrete cracks form, and spalling may occur [26, 27]. Park and Paulay [28] pointed out that a column's total displacement can be characterised by its curvature and height, as well as the length of the yielding region. In the different specimens, the strain in the steel reinforcements accumulated and localized differently. Figure 12 shows the first yielding-recorded displacements and crack localization of the specimens. Compared to the conventional concrete specimens, the reinforced ECC specimens displayed more fine cracks and plastic deformation, leading to differences in the normalized energy dissipated per cycle of the specimens. The length of the plastic hinge presented in Table 6 is based on the strain gauge data, considered when monitoring the strain of the longitudinal bars and the surface of the specimen. The data showed that the length of the plastic joint changes from one to two by increasing the aspect ratio and fibre percentage. Figure 13 shows the different lengths of plastic zones in SP4 and SP5. The distribution of micro-cracks was greater in SP12, SP11, SP10, and SP9 than in SP7, SP6, and SP4.

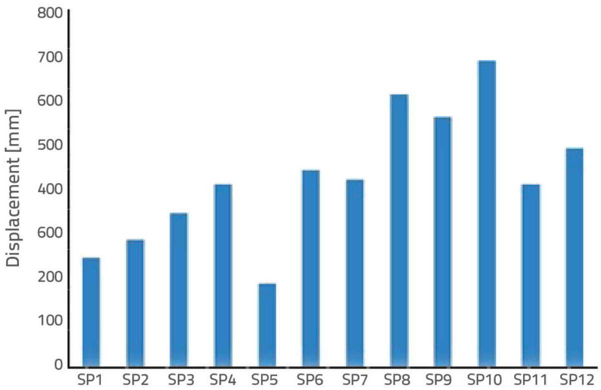

Figure 12. Yielding displacement of longitudinal reinforcement

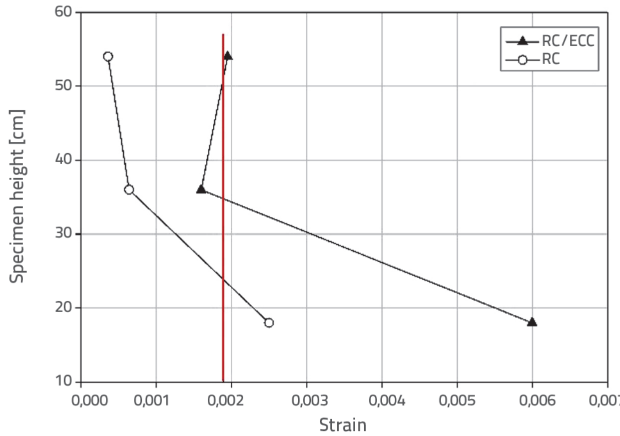

Figure 13. Plastic hinge length in SP4 (ECC) and SP5 (RC)

Table 6. Length of the plastic hinge

Aspect ratio	Fibre fraction	Plastic region
3	0-0.3 %	1.0 D*
5	0.6 %	1.5 D*
7	1-1.5 %	2 D*
D* represents the dimension of the column		

4. Conclusions

In this study, 12 square column specimens (one made from conventional concrete and 11 made from ECCs with different fibre fractions and aspect ratios) were evaluated to investigate the effects of using ECCs on the seismic performance of column components. The findings of this study are summarized below:

- The failure mode changed from crack localization to strain-hardening by increasing the aspect ratio and fibre fraction.
- The reinforced ECC specimens dissipated more energy than the reinforced concrete specimens. They also exhibited a higher ultimate drift and more resistance to splitting and spalling with the same amount of transverse steel reinforcement. The cumulative energy dissipation capacity of the ECC column was approximately 100 % higher than that of the conventional concrete column.
- The cumulative energy dissipation capacity of ECCs was higher than that of conventional concrete and increased with the fibre volume fraction.
- The proper performance and bridging of the fibres were observed in the distribution of shear in the ECC specimens, while the transverse bars remained elastic.
- The ECC columns had longer yield regions than the conventional concrete column; increasing the aspect ratio and fibre volume fraction of the ECC columns intensified this difference.
- The drift capacity of the ECC columns improved by increasing the aspect ratio and fibre fraction.

REFERENCES

[1] Yang, E., Li, V.C.: Numerical study on steady-state cracking of composites. Composites Science and Technology, 67 (2007) 2, pp. 151–156.

[2] Ranade, R., Li, V.C., Stults, M.D., Rushing, T.S., Roth, J., Heard, W.F.: Micromechanics of high-strength, high-ductility concrete. ACI Materials Journal, 110 (2013) 4, pp. 375–384.

[3] Lu, C., Leung, C.K.Y.: Theoretical evaluation of fiber orientation and its effects on mechanical properties in engineered cementitious composites (ECC) with various thicknesses. Cement and Concrete Research, 95 (2017), pp. 240–246.

[4] Li, V.C., Wang, Y., Backer, S.: Effect of inclining angle, bundling and surface treatment on synthetic fibre pull-out from a cement matrix. Composites, 21 (1990) 2, pp. 132–140.

[5] Ismail, M.K., Abdelaleem, B.H., Hassan, A.A.A.: Effect of fiber type on the behavior of cementitious composite beam-column joints under reversed cyclic loading. Construction and Building Materials, 186 (2018), pp. 969-77.

[6] Shao, Y., Billington, S.L.: Predicting the two predominant flexural failure paths of longitudinally reinforced high-performance fiber-reinforced cementitious composite structural members. Engineering Structures, 199 (2019), pp. 109581.

[7] Fukuyama, H., Matsuzaki, Y., Sato, Y., Iso, M., Suwada, H.: Structural Performance of Engineered cementitious composite elements, composite and hybrid structures, 6th ASCCS International Conference on Steel-Concrete Composite Structures, pp. 969–976, 2000.

[8] Parra-Montesinos, G., Wight, J.K.: Seismic response of exterior RC column-to-steel beam connections. Journal of Structural Engineering 126 (2000), pp. 1113–1121.

[9] Fischer, G., Li, V.C.: Intrinsic response control of moment-resisting frames utilizing advanced composite materials and structural elements. ACI Structural Journal, 100 (2003) 2, pp. 166–176.

[10] Kang, S.-B., Tan, K.H., Zhou, X.-H., Yang, B.: Influence of reinforcement ratio on tension stiffening of 506 reinforced engineered cementitious composites. Engineering Structures, 141 (2017), pp. 251-62.

[11] Moreno, D.M., Trono, W., Jen, G., Ostertag, C., Billington S.L.: Tension stiffening in reinforced high performance fiber reinforced cement-based composites. Cement and Concrete Composites, 50 (2014), pp. 36–46.

[12] Fischer, G., Li, V.C.: Influence of matrix ductility on tension-stiffening behavior of steel reinforced engineered cementitious composites (ECC). ACI Structural Journal, 99 (2002), pp. 104–11.

[13] Shao, Y., Billington, S.L.: Predicting the two predominant flexural failure paths of longitudinally reinforced high-performance fiber-reinforced cementitious composite structural members. Engineering Structures, 199 (2019), pp. 109581.

[14] Bandelt, M.J., Billington, S.L.: Impact of reinforcement ratio and loading type on the deformation capacity of high-performance fiber-reinforced cementitious composites reinforced with mild steel. Journal of Structural Engineering 142 (2016), pp. 14.

[15] Fischer, G., Li, V.C.: Effect of matrix ductility on deformation behavior of steel-reinforced ECC flexural members under reversed cyclic loading conditions. ACI Structural Journal, 99 (2002), pp. 781–90.

[16] Frank, T.E., Lepech, M.D., Billington, S.L.: Experimental testing of reinforced concrete and reinforced ECC flexural members subjected to various cyclic deformation histories. Materials and Structures, 50 (2017), pp. 232.

[17] Lepech, M.D., Li, V.C.: Application of ECC for bridge deck link slabs. RILEM J. Mater. Struct. 42(9), 1185–1195 (2009)

[18] JSCE.: Recommendations for design and construction of high performance fiber reinforced cement composites with multiple fine cracks (HPFRCC), Japan, 2008.

[19] ACI 374.2R-13: American Concrete Institute. Guide for testing reinforced concrete structural elements under slowly applied simulated seismic loads, 2013.

[20] Moreno, D.M., Trono, W., Jen, G., Ostertag, C., Billington, S.L.: Tension stiffening in reinforced high performance fiber reinforced cement-based composites. Cement and Concrete Composites, 50 (2014), pp. 36–46.

[21] Yoo, D.Y., Yoon, Y.S.: Structural performance of ultra-high-performance concrete beams with different steel fibers. Engineering Structures, 102 (2015), pp. 409–23.

[22] Ding, Y., Yu, K.Q., Yu, J.T., Xu, S.L.: Structural behaviors of ultra-high performance engineered cementitious composites (UHP-ECC) beams subjected to bending-experimental study. Construction and Building Materials, 177 (2018), pp. 102–15.

[23] Bandelt, M.J., Billington, S.L.: impact of reinforcement ratio and loading type on the deformation capacity of high-performance fiber-reinforced cementitious composites reinforced with mild steel. Journal of Structural Engineering, 142 (2016), pp. 14.

[24] Kanda, T., Watanabe, S., Li, V.C.: Application of Pseudo strain hardening cementitious composites to shear resistant structural elements. FRAMCOS-3 (1998), pp. 1477–1490.

[25] ASCE standard ASCE/SEI 41-13 : American Society of Civil Engineers : seismic evaluation and retrofit of existing buildings.

[26] Mortezaei, A.: Plastic hinge length of RC columns under the combined effect of near-ault vertical and horizontal ground motions. Periodica Polytechnica Civil Engineering, 58 (2014) 3, pp. 243–53.

[27] Mortezaei, A.: Plastic hinge length of RC columns considering soil-structure interaction, Earthquakes and Structures, 5 (2013) 6, pp. 679-702

[28] Park, R., Paulay, T.: Reinforced concrete structures. John Wiley & Sons, 1975.